

# **Micro-Composite Fabrication via Field-Aided Laminar Composite (FALCom) Processing**

**by Larry R. Holmes, Jr.**

**ARL-TR-6106**

**September 2012**

## **NOTICES**

### **Disclaimers**

The findings in this report are not to be construed as an official Department of the Army position unless so designated by other authorized documents.

Citation of manufacturer's or trade names does not constitute an official endorsement or approval of the use thereof.

Destroy this report when it is no longer needed. Do not return it to the originator.

# **Army Research Laboratory**

Aberdeen Proving Ground, MD 21005-5069

---

**ARL-TR-6106****September 2012**

---

## **Micro-Composite Fabrication via Field-Aided Laminar Composite (FALCom) Processing**

**Larry R. Holmes, Jr.**  
**Weapons and Materials Research Directorate, ARL**

REPORT DOCUMENTATION PAGE				Form Approved OMB No. 0704-0188	
Public reporting burden for this collection of information is estimated to average 1 hour per response, including the time for reviewing instructions, searching existing data sources, gathering and maintaining the data needed, and completing and reviewing the collection information. Send comments regarding this burden estimate or any other aspect of this collection of information, including suggestions for reducing the burden, to Department of Defense, Washington Headquarters Services, Directorate for Information Operations and Reports (0704-0188), 1215 Jefferson Davis Highway, Suite 1204, Arlington, VA 22202-4302. Respondents should be aware that notwithstanding any other provision of law, no person shall be subject to any penalty for failing to comply with a collection of information if it does not display a currently valid OMB control number. <b>PLEASE DO NOT RETURN YOUR FORM TO THE ABOVE ADDRESS.</b>					
1. REPORT DATE (DD-MM-YYYY) September 2012		2. REPORT TYPE Final		3. DATES COVERED (From - To) January 2008 to present	
4. TITLE AND SUBTITLE Micro-Composite Fabrication via Field-Aided Laminar Composite (FALCom) Processing				5a. CONTRACT NUMBER	
				5b. GRANT NUMBER	
				5c. PROGRAM ELEMENT NUMBER	
6. AUTHOR(S) Larry R. Holmes, Jr.				5d. PROJECT NUMBER MMCP04B	
				5e. TASK NUMBER	
				5f. WORK UNIT NUMBER	
7. PERFORMING ORGANIZATION NAME(S) AND ADDRESS(ES) U.S. Army Research Laboratory ATTN: RDRL-WMM-A Aberdeen Proving Ground, MD 21005-5069				8. PERFORMING ORGANIZATION REPORT NUMBER ARL-TR-6106	
9. SPONSORING/MONITORING AGENCY NAME(S) AND ADDRESS(ES)				10. SPONSOR/MONITOR'S ACRONYM(S)	
				11. SPONSOR/MONITOR'S REPORT NUMBER(S)	
12. DISTRIBUTION/AVAILABILITY STATEMENT Approved for public release; distribution is unlimited.					
13. SUPPLEMENTARY NOTES					
14. ABSTRACT A novel composite fabrication process is used to create multi-functional micro-composites, which can be tailored for specific end-use applications. The Field-Aided Laminar Composite (FALCom) process uses specifically focused electric fields to align nano- to micro-sized particles into chain-like structures, which are referred to as pseudo-fibers. These pseudo-fibers are then immediately frozen into place by the laser curing of the photopolymer matrix. The pseudo-fibers are arranged by design, and are used to create three-dimensional composite structures. In this research, multiple filler particles were selected for processing evaluation. Multi-walled carbon nano-tubes, aluminum micro-particles, and alumina micro-particles were aligned and oriented in an acrylic photopolymer matrix. Examples of processing and a review of experimental processing are shown, and conclusions and future work are discussed.					
15. SUBJECT TERMS composite processing, composite fabrication, micro-composite, rapid prototyping					
16. SECURITY CLASSIFICATION OF:			17. LIMITATION OF ABSTRACT  UU	18. NUMBER OF PAGES 30	19a. NAME OF RESPONSIBLE PERSON Larry R. Holmes, Jr.
a. REPORT Unclassified	b. ABSTRACT Unclassified	c. THIS PAGE Unclassified			19b. TELEPHONE NUMBER (Include area code) 410-306-4951

---

## Contents

---

<b>Contents</b>	<b>iii</b>
<b>List of Figures</b>	<b>iv</b>
<b>List of Tables</b>	<b>v</b>
<b>Acknowledgments</b>	<b>vi</b>
<b>1. Introduction</b>	<b>1</b>
<b>2. Experimentation</b>	<b>2</b>
2.1 Materials .....	2
2.1.1 Filler Selection .....	2
2.1.2 Resin Selection .....	3
2.2 Material Processing .....	3
2.2.1 Filler Content.....	3
2.2.2 Filler Dispersion .....	4
2.3 Electric Field Particle Alignment .....	7
2.3.1 Background .....	7
2.3.2 Processing Times Based on Alignment Variables .....	8
2.4 Experimental Apparatus and Process .....	10
<b>3. Results and Conclusions</b>	<b>16</b>
<b>4. References</b>	<b>18</b>
<b>Distribution List</b>	<b>20</b>

---

## List of Figures

---

Figure 1. TEM image of cross-sections of MWCNTs.....	2
Figure 2. Digital microscope image of aluminum micro-particles, circled particles average ~50 $\mu\text{m}$ . .....	3
Figure 3. Image of mixing apparatus' including: 1. Silverson high shear mixer, 2. Branson ultrasonic bath and 3. Fisher Scientific magnetic hot-plate. ....	5
Figure 4. Images of well dispersed particles (left) compared to particles mixed by magnetic stir bar only (right): 1. Aluminum micro-particles, 2. Alumina micro-particles, 3. MWCNTs.....	6
Figure 5. A high aspect ratio, non-uniform particle experiencing torque imposed by an electric field $\mathbf{E}$ . .....	7
Figure 6. Polarized particles in electric fields forming chains.....	8
Figure 7. General mechanism setup for all experiments.....	11
Figure 8. Processing area and electrode alignment for initial experimentation.....	12
Figure 9. Schematic of laser and UV mold movements. ....	12
Figure 10. Image of the laser system for the photopolymer experiments.....	13
Figure 11. Image of initial FALCom processing apparatus.....	13
Figure 12. Images of UV photopolymer samples, (l-r): sample with bi-directional alignment and sample with uni-directional alignment. ....	14
Figure 13. Images of a bi-directional sample taken by a digital microscope, (c.w. from top left): $0^\circ$ orientation, $90^\circ$ orientation, bi-directional alignment overlapping view .....	15
Figure 14. Laminar micro-composite; aluminum micro-particles aligned in a $0^\circ$ , $90^\circ$ orientation in an acrylic matrix. ....	16
Figure 15. Example of photoelastic response of a unidirectional micro-composite with carbon particulate chains in an acrylic matrix. An arrow denotes direction of alignment. ....	17

---

## List of Tables

---

Table 1. Rheometric testing of filler-photopolymer mixtures; viscosities at 1.0 weight-percent of filler.....	4
Table 2. Summary of selected materials with filler percent by weight. ....	4
Table 3. Theoretical processing times based on alignment variables $\mathbf{E}$ and $\eta$ (18, 19).....	9
Table 4. Theoretical processing times of epoxy with varying electrode distances (18, 19).....	10

---

## Acknowledgments

---

This investigation was accomplished through the support of many U.S. Army Research Laboratory colleagues. In particular, I would like to thank Jared Gardner and Zach Larimore for their assistance and input. I would also like to thank Dr. Tom Turng, University of Wisconsin-Madison, for his leadership and support.



---

## 1. Introduction

---

In the late 1800s, J.C. Maxwell developed the fundamental laws of electromagnetism, which are used to explain the functions of both electric and magnetic fields. However, it was not until the 1950's that H. Pohl reported his discovery that particles in a dielectric fluid experience forces when placed in an electric field. One of these forces was named dielectrophoresis, and is defined as the translational motion of neutral matter caused by polarization effects in a non-uniform electric field (1–4).

Much work has been accomplished since Pohl's discovery, including: mathematical descriptions of the forces and resulting motion of particles of differing shapes, particle separation and segregation for use in drug delivery, and even the manipulation of long-chain molecules of certain polymers. See references (5–10) for a more complete description of these studies.

Recently, researchers at the University of Wisconsin-Madison have developed a technology called Field-Aided Micro-Tailoring (FAiMTa) (11–14). FAiMTa uses a liquid polymer solution containing nano- to micro-sized particles that is cured in the presence of an electric field. This produces a solid structure with fillers aligned in a particular direction, according to the orientation of the electric field. Kim (11, 13) also defines processing characteristics by describing particle manipulation times as a function of electric field strength.

The research presented here builds upon the FAiMTa technology in the design of a processing system that allows for nano- to micro-scale fillers to be aligned and oriented in a liquid photopolymer solution before being locked in place by the laser curing of the photopolymer matrix. The Field-Aided Laminar Composite (FALCom) processing technology is the realization of this research. Using FALCom processing, fillers are aligned into pseudo-fibers that can be arranged by design. Systems can then be designed with structural, thermally conductive, or electrically conductive fillers for multifunctional applications, which will allow for the production of three-dimensional composites for structural, electrical, or heat sink applications.

It is shown here that a combination of properly controlled electric fields and accurate material selection can lead to functionally graded composite materials with locally tailored filler modifications by design (1).

---

## 2. Experimentation

---

### 2.1 Materials

#### 2.1.1 Filler Selection

In order to test multiple fabrication scenarios, fillers were selected based on particle size and material characteristics. The lower limit of the size range tested was 20 nm which was selected in order to compare processing results to previous research by Rud (*14*). The upper limit of the size range tested was 80  $\mu\text{m}$ . At 80  $\mu\text{m}$ , the particles are small enough that multiple particles can be manipulated by the electric field at one time, and the resulting aligned pseudo-fibers are large enough to see with the human eye, which allows for ease in experimental processing. Fillers were also chosen so as to represent a broad range of materials, in this case, metals, ceramics, and nano-organics.

Multi-walled carbon nanotubes (MWCNTs), aluminum micro-particles, and alumina micro-particles were selected because they meet the above criteria, and are easily obtained through commercial sources.

The MWCNTs used here were acquired from Carbon Nanotechnologies Inc, a distributor for Unidym, Inc. (Sunnyvale, CA). An image of the MWCNTs taken by transmission electron microscope (TEM) can be seen in figure 1. In the image, the ring-like structures are the cross-sectional ends of the MWCNTs (*1*).

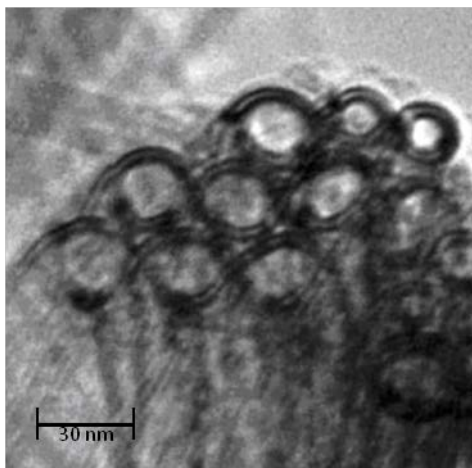


Figure 1. TEM image of cross-sections of MWCNTs.

The alumina micro-particles used in this study were captured from a milling process and have a particle size range of 45 to 53  $\mu\text{m}$  (*1*).

The aluminum micro-particles used in this study were acquired from West Systems (Bay City, MI), and have a particle size between 20 and 50  $\mu\text{m}$ . An image of these particles, seen in figure 2, was taken with a Zeiss Stemi 200-C laboratory microscope with Pulnix AccuPiXEL digital output (1).

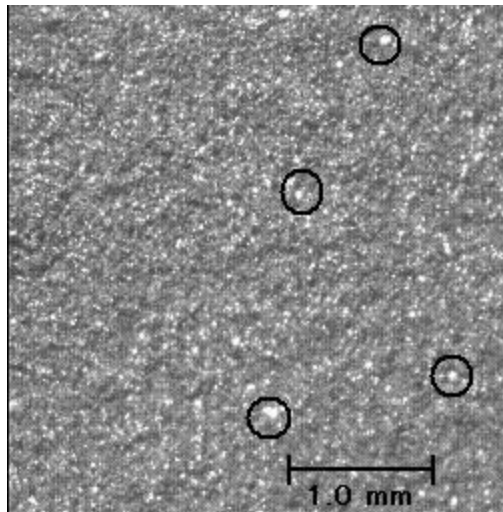


Figure 2. Digital microscope image of aluminum micro-particles, circled particles average  $\sim 50 \mu\text{m}$ .

### 2.1.2 Resin Selection

An ultra-violet (UV) curable acrylate photopolymer system formulated by Allied Photo Chemical (Kimball, MI) was used as the matrix material in this study. This material is transparent, which makes viewing particle alignment possible. From Kim (11, 13), it was determined that the matrix material would need to have a viscosity under 1000 cP in order for alignment to take place in a short time scale. The photopolymer used here has a viscosity of 900 cP at room temperature. These characteristics were easily extracted, and met the criteria necessary for this project. However, one major concern was that the matrix material needs to be non-conductive in its liquid pre-cured state. Allied Photo Chemical specifically designed this acrylate system to contain non-conductive photoinitiators, which allowed for the liquid polymer to be non-conductive (1).

## 2.2 Material Processing

### 2.2.1 Filler Content

Initial experimentation was conducted with 0.1 volume-percent MWCNTs in an epoxy matrix in order to replicate the work by Rud (14), and to verify the test apparatus discussed later. While mixing these materials, it was discovered that the liquid polymer viscosity increased dramatically with the addition of MWCNTs in amounts more than 0.5 weight-percent. A TA Instruments Advanced Rheometer AR-1000 was used to determine the viscosity of the mixtures, and to

verify the drastic change in viscosity. Samples of 1.0 weight-percent filler mixtures from each of three sample sets were evaluated with the liquid photopolymer, and the resulting viscosities are shown in table 1.

Table 1. Rheometric testing of filler-photopolymer mixtures; viscosities at 1.0 weight-percent of filler.

<b>Filler Material at 1.0 Weight-Percent</b>	<b>Viscosity cP</b>
Control (no filler)	900
Aluminum	930
Alumina	960
MWCNTs	8300

From the information in table 1, it can be seen that the mixture of 1.0 weight-percent of MWCNTs dramatically increases the viscosity of the photopolymer. This viscosity is well above the processing viscosity of 1000 cP, determined during material selection. To continue testing the possibilities of MWCNT alignment in these experiments, it was determined that only small amounts (less than 0.1 weight-percent) of MWCNTs could be used while maintaining a workable polymer viscosity of 917 cP. Final sample sets for experimental processing included 0.3 and 1.0 weight-percent of aluminum micro-particles and alumina micro-particles and less than 0.1 weight-percent MWCNTs. A summary of the sample mixtures along with the percentage of fillers by weight used can be seen in table 2.

Table 2. Summary of selected materials with filler percent by weight.

<b>Filler Materials</b>	<b>Filler Sizes</b>	<b>Filler Percentages</b>
MWCNTs	40–70 nm	0.1 wt %
Aluminum	20–50 $\mu\text{m}$	0.3 wt %, 1.0 wt %
Alumina	45–53 $\mu\text{m}$	0.3 wt %, 1.0 wt %

### 2.2.2 Filler Dispersion

Samples undergo a series of mixing and degassing steps in order to create a solution with well distributed fillers which are free of trapped gasses. Mixing equipment includes a Silverson L4RT high-shear mixer, a Fisher Scientific Isotemp magnetic hot plate, and a Branson 2510 ultrasonic bath. The mixture is placed in a Fisher Scientific Isotemp 280A vacuum oven at a constant temperature of 100 °C and a constant vacuum of ~29 in of Mercury. This is done in order to remove the gas from the sample which is often added during the mixing process. Once

the mixture has been degassed it is ready for processing. Figure 3 shows an image of the apparatus' used for mixing.



Figure 3. Image of mixing apparatus' including:  
1. Silverson high shear mixer, 2. Branson ultrasonic bath and 3. Fisher Scientific magnetic hot-plate.

Initially, the fillers are hand mixed into the liquid polymer in order to assure the fillers fully wet out and are not left as dry clumps in the liquid. All solutions are then mixed with magnetic stir plate to assure the fillers do not fall out of solution. The solution with MWCNTs then undergoes high shear mixing. The high shear mixing is necessary for the proper distribution of the MWCNTs in most any liquid matrix due to large Van der Waals forces caused by the relatively large interface for the nanotubes to aggregate (15). This step is not necessary for the micro-particles used in this experiment because the micro-particles have a much smaller relative surface area and, therefore, less Van der Waals forces.

All filler-polymer solutions are then sonicated in an ultrasonic bath, and then moved into a vacuum oven for degassing. Figure 4 shows images of well dispersed mixtures as compared to mixtures by magnetic stir rod only. The images below show that the aluminum and alumina micro-particle mixtures that were mixed with only the stir bar have larger particle agglomerates and have darker areas that appear to have higher concentrations of particles.

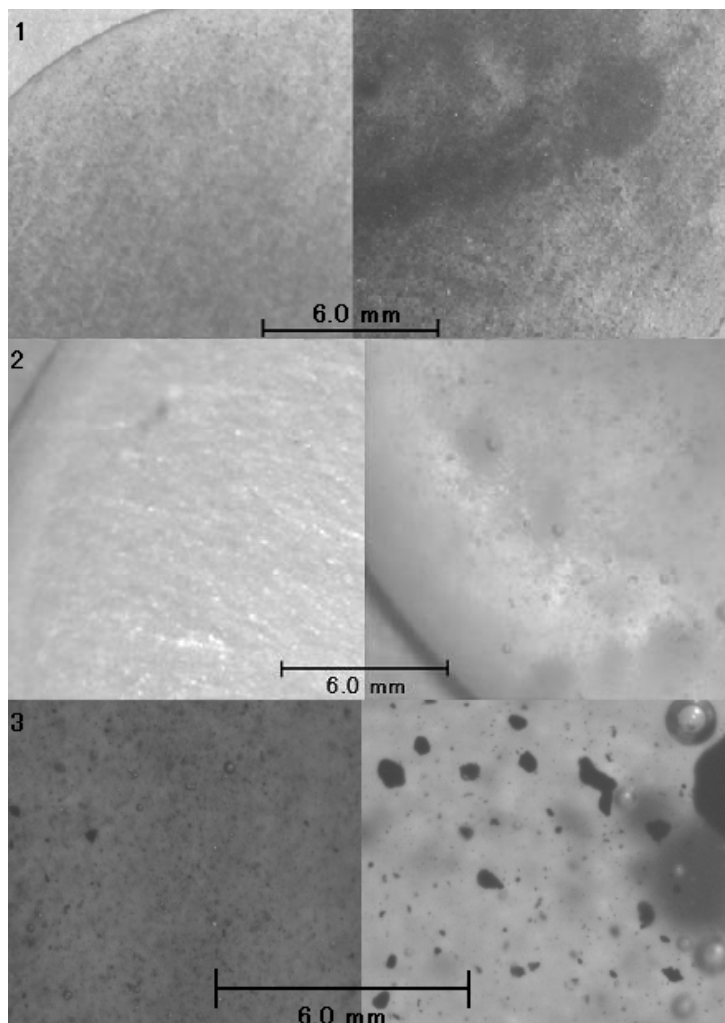


Figure 4. Images of well dispersed particles (left) compared to particles mixed by magnetic stir bar only (right):  
 1. Aluminum micro-particles, 2. Alumina micro-particles, 3. MWCNTs.

The MWCNT mixture that only underwent stir bar mixing has much larger particle agglomerates and appears clearer than that of the mixture that underwent the entire dispersion procedure. The clarity is due to agglomeration, having less light blocked because of low dispersion. All of the samples that were mixed using the stir bar also seem to contain bubbles that were almost totally removed during degassing of the mixed solutions. The MWCNT mixtures used in this study still contained agglomerated particles but at a much lower concentration than that of the magnetic stir bar sample.

## 2.3 Electric Field Particle Alignment

### 2.3.1 Background

When a dielectric material is placed in an electric field, it will be polarized with the dipole moment,  $\mu$ , proportional to the applied electric field,  $\mathbf{E}$ , as,

$$\mu = \alpha \cdot \mathbf{E}, \quad (1)$$

where  $\alpha$  is the polarizability tensor. For a spherical particle, the dipole moment is parallel to applied electric field, namely,

$$\mu = 3V \epsilon_0 (\epsilon_p - \epsilon_c) \beta E, \quad (2)$$

with the dipole coefficient,

$$\beta = \frac{\epsilon_p - \epsilon_c}{\epsilon_p + 2\epsilon_c}, \quad (3)$$

where  $V$  is the particle volume.  $\epsilon_0$  is the dielectric constant of free space;  $\epsilon_p$  and  $\epsilon_c$  are the relative dielectric constant of the particle and the continuous media in which the particle is placed, respectively.

For a non-spherical particle, the dipole moment is not necessarily parallel to the applied electric field, which induces a torque,  $\mathbf{T}$ , aligning the particle in the electric field direction (16),

$$\mathbf{T} = \mu \times \mathbf{E}. \quad (4)$$

Figure 5 shows a high aspect ratio fiber experiencing torque imposed by an electric field  $\mathbf{E}$ . Detailed mathematical descriptions of non-spherical particles in an electric field are referred to in publications by Kim (17–19).

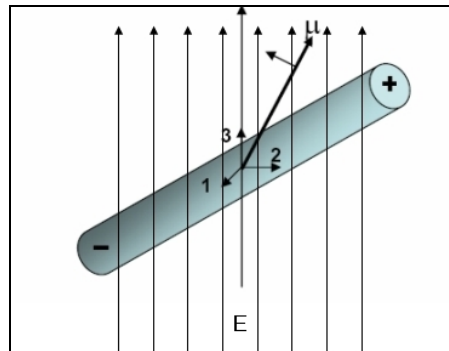


Figure 5. A high aspect ratio, non-uniform particle experiencing torque imposed by an electric field  $\mathbf{E}$ .

Known as the electrophoresis phenomenon, a suspended charged particle migrates under the influence of an applied electric field because the electric field exerts an electrostatic Coulomb force,  $\mathbf{F}$ , on the particle through the charge,  $q$ , which it carries,

$$\mathbf{F} = q\mathbf{E} \quad (5)$$

This force moves the particle to the electrode with the opposite charges. The motion of a non-charged particle in a non-uniform electric field is called dielectrophoresis, which is caused by polarization effects. The force acting on a dielectric particle in a non-uniform electric field is,

$$\mathbf{F} = (\mu \bullet \nabla)\mathbf{E} \quad (6)$$

This force moves the particle towards the stronger field region.

When more than two particles are placed in an applied electric field, the electric field around one particle is disturbed by the electric fields generated by all surrounding particles, which leads to attractive and repulsive forces between the inclusions. The dipole-dipole interactions adjust the relative position of neighboring particles and align them along the electric field direction. Figure 6 shows that the polarized particles form chains parallel with the imposed electric field (16–19).

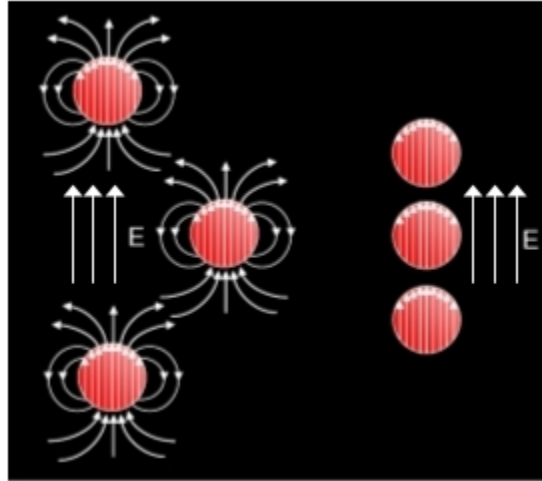


Figure 6. Polarized particles in electric fields forming chains.

### 2.3.2 Processing Times Based on Alignment Variables

In these experiments, an electric field is used to induce a force on fillers suspended in a liquid polymer matrix. As discussed before, this induced force creates a torque on the individual particles in the mixture. The applied torque then rotates the particle in order for the particle to align with the direction of the electric field and to create chain-like structures or pseudo-fibers. The electric-field induced force and torque along with the Stoke's drag equations can be used to determine the rotation and alignment times of particles in a fluid. Equations 7 and 8 give the



estimated time it takes to rotate a high aspect ratio fiber and to align particles in a chain, respectively. These times are dependant of the fluid viscosity,  $\eta$ , and the square of the electric field strength,  $E$  (17–19).

Time for an electric field to rotate a high aspect ratio particle is

$$t_{rotate} \approx 10^2 \eta / \epsilon_0 E^2. \quad (7)$$

Time for an electric field to align particle chains is,

$$t_{chain} \approx 10 \eta / \epsilon_0 E^2. \quad (8)$$

From the equations above, Kim predicted processing times for various matrix materials (18, 19). Table 3 gives predicted processing times of particles in various matrices based on the magnitude of the electric field and matrix viscosities.

Table 3. Theoretical processing times based on alignment variables  $E$  and  $\eta$  (18, 19).

Materials	Viscosity (Poise)	Processing Times at 10 kV/mm (s)	Processing Times at 1 kV/mm (s)
Low density polyethylene	3160	3	300
Polystyrene	10000	10	1020
Polypropylene	10000	10	1020
Polycarbonate	3160	3	300
Polyamide	700	0.7	66
Poly(ethylene terephthalate)	1000	1	96
Epoxy with hardener	0.7	0.007	0.7

The matrix viscosity is a major dynamic in this process. However, it can be seen from table 3 that the electric field strength is the most significant variable in the system. The theoretical values given by Kim show promise for electric field alignment to be used in some types of polymer processing, however, due to voltage amplifier restrictions in these experiments, only a peak-to-peak voltage ( $V_{p-p}$ ) of 800 V is possible for a 1 mm long span. Table 4 shows processing times for an epoxy system (with rheological properties like the photopolymer used in this study) based on the attainable 800  $V_{p-p}$  with varying distances between electrodes.

Table 4. Theoretical processing times of epoxy with varying electrode distances (18, 19).

Varying Voltage per Electrode Distance	Processing Times of Epoxy (0.7 Poise)	Distance Between Electrodes
10 kV/mm	0.007	NA
1k V/mm	0.7	NA
800 V/mm	1.1	1 mm
400 V/mm	4.375	2 mm
200 V/mm	17.5 s	4 mm
100 V/mm	70 s	8 mm
50 V/mm	280	16 mm

## 2.4 Experimental Apparatus and Process

The experimental setup in this study consists of a GW-Instek GFG-8015G function generator, a GW-Instek GDS-820C digital oscilloscope, and a Trek 609D-6 high voltage amplifier. The function generator is the mechanism that produces the signals used to create the electric field. For these experiments, the function generator is set to produce a sinusoidal signal. The voltage output and frequency output of the function generator are sent to the oscilloscope and to the voltage amplifier. The voltage amplifier magnifies the voltage input from the function generator by one thousand times, and then sends out a signal voltage to electrodes. The oscilloscope is used to monitor the frequencies and voltages of the function generator and voltage amplifier. The electrodes are then placed in desired locations in order to perform particle alignment by design. Visual verification of particle alignment in semi-transparent samples is done by the Zeiss Stemi 2000-C microscope with a Pulnix AccuPiXEL digital output. Figure 7 shows an image of the described equipment.

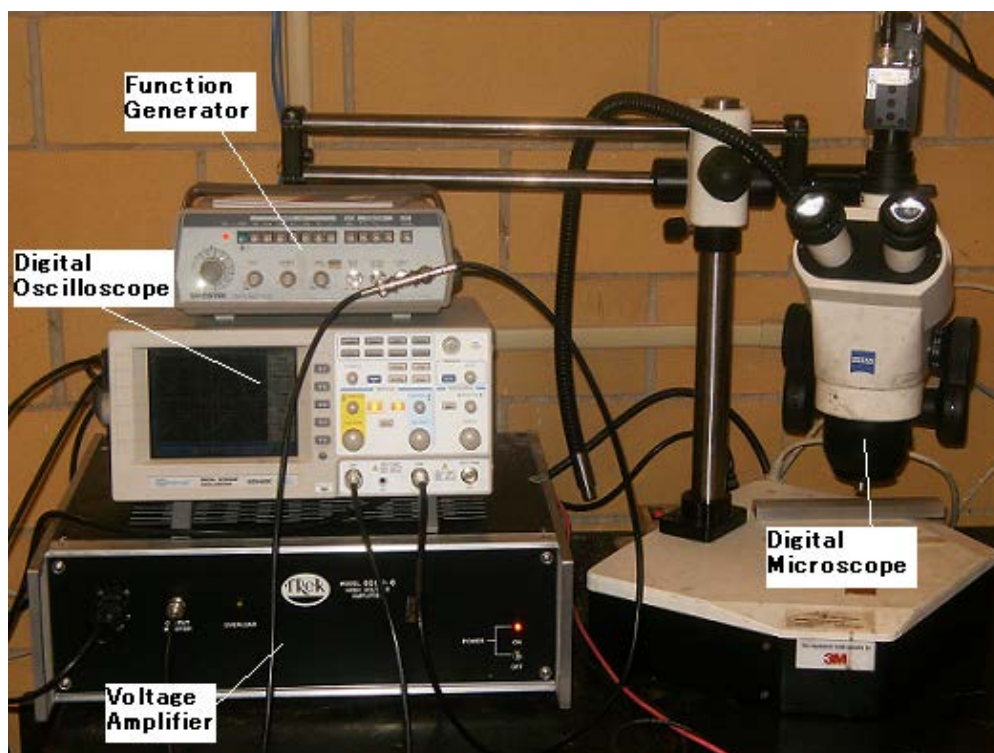


Figure 7. General mechanism setup for all experiments.

It should be noted that in all of the experiments, the electrodes have been insulated from the samples being created by a thin layer of polycarbonate. Insulation of the electrodes is necessary when using electrically conductive filler materials, because as the chains or pseudo fibers are formed, the circuit can be completed within the material causing a short.

The processing area for testing the materials and equipment in this experiment can be seen in figure 8. Here, the electrodes are in parallel alignment and are designed to align the MWCNTs through the width of the epoxy matrix. Large agglomerates of MWCNTs were left in this sample experiment for ease of tracking particle motion. A picture of the specimen being aligned, taken with the digital microscope, can be seen in the inset of the figure.

Once tests were conducted and particle alignment was verified, an apparatus was built in order to align particles and cure the matrix at desired locations, which marked the development of the FALCom processing technology. The function generator, oscilloscope, and voltage amplifier are used in the same manner as before; however, the electrodes are placed in parallel plate alignment on a rectangular mold. The mold, which contains the solution of filler and photopolymer, rests on a glass plate which covers a hole in a laboratory table with a non-conductive surface. Under the table is the UV laser emitter. The laser emitter and mold are able to move back and forth, perpendicular to one another. This allows for the laser to be able to cure all desired areas of the sample. The mold and laser movements are controlled by electric motor crank-axel gearboxes. A schematic of the mold and laser motion is depicted in figure 9.

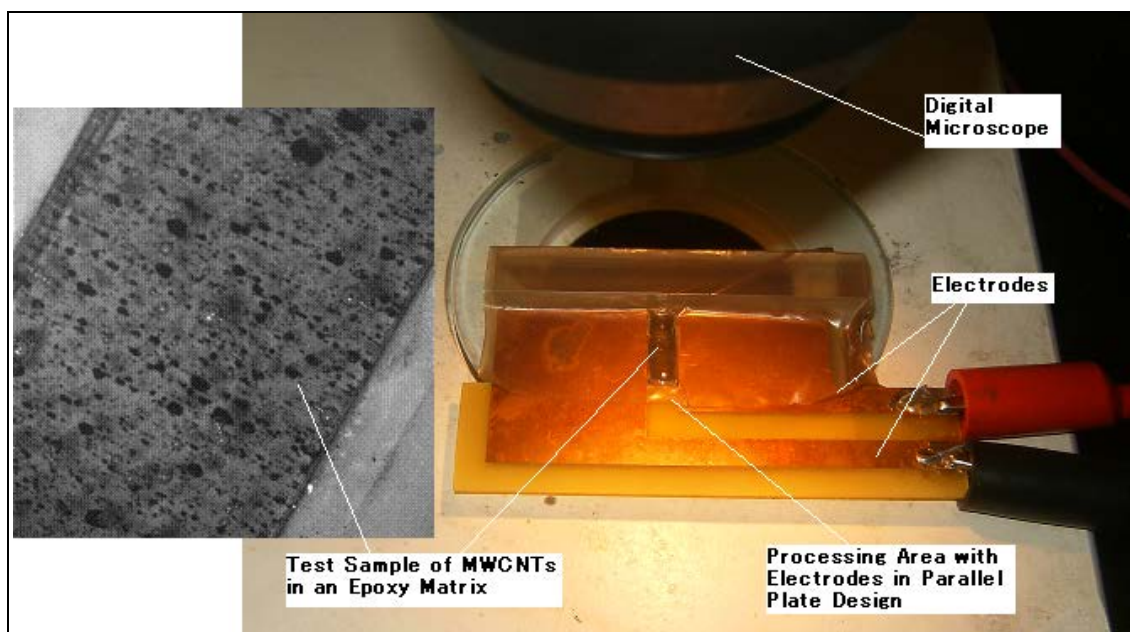


Figure 8. Processing area and electrode alignment for initial experimentation.

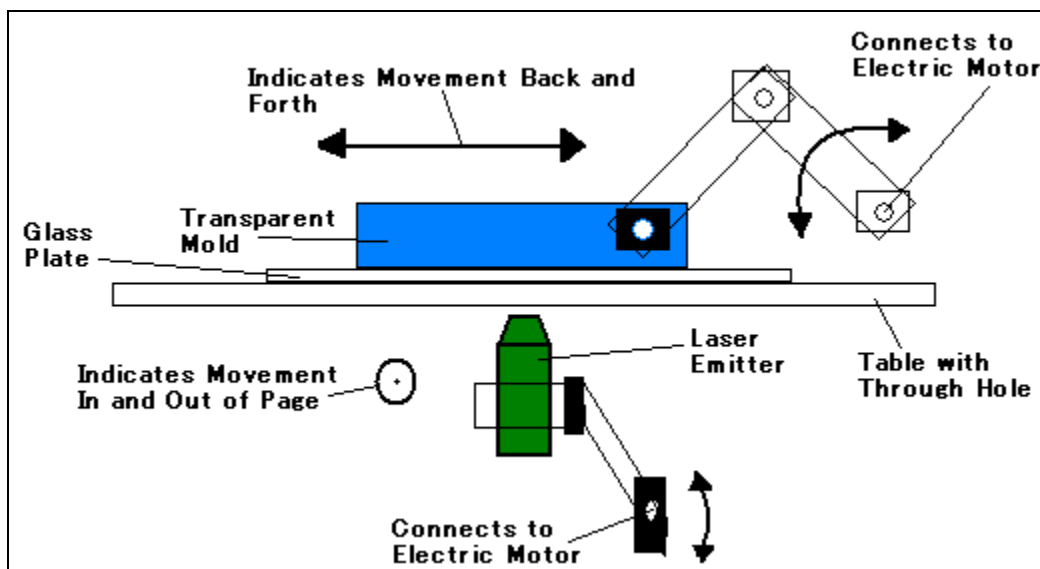


Figure 9. Schematic of laser and UV mold movements.

The laser emits a UV beam from a UV Source, Inc., Green Spot laser system. The laser is used to cure the photopolymer composite after particle alignment. Figure 10 shows an image of the laser system for the UV photopolymer experiments, and figure 11 shows the first FALCom apparatus.



Figure 10. Image of the laser system for the photopolymer experiments.

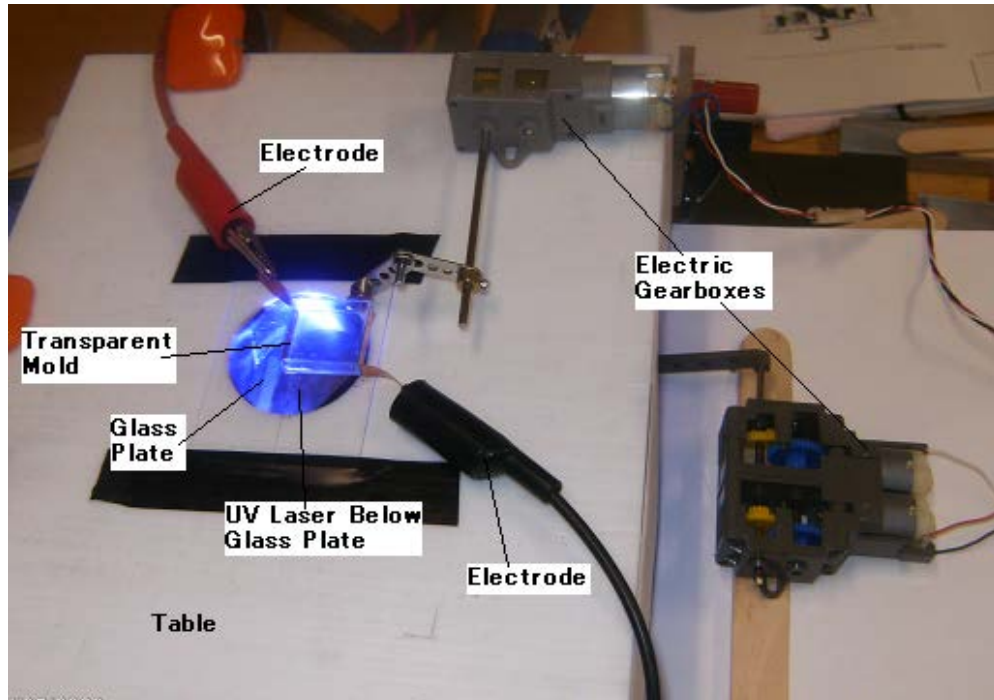


Figure 11. Image of initial FALCom processing apparatus.

In this image, the transparent polymer composite being fabricated is in the transparent mold. The electrodes are used to align the fillers perpendicular to their surfaces. After alignment, the material is cured as the mold moves side to side (left to right in this picture) the laser under the glass plate moves in a perpendicular direction there by allowing for the laser to cure all areas of the mold. The gearbox connected to the mold simply rotates the axel from  $0^\circ$  (position in the picture) to  $45^\circ$  and then back to  $0^\circ$ . This allows the mold to travel across the glass plate. The gearbox controlling the laser also moves its axel from  $0^\circ$  (position in picture) to  $45^\circ$  and then

back again. The lever arm on the laser gearbox is connected to a spiral bevel gear that is connected to the laser emitter by another lever arm. This moves the laser in the opposite direction as the motion of the transparent mold.

The particle alignment for these experiments is based on parallel plate design, with the fillers being aligned through the width of the parts in both uni-directional and bi-directional patterns. Figure 12 shows images of sample specimens made for both alignment setups.

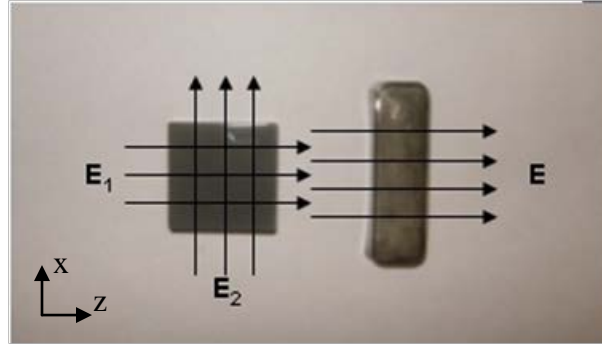


Figure 12. Images of UV photopolymer samples, (l-r): sample with bi-directional alignment and sample with uni-directional alignment.

In the images above, the uni-directional sample (rectangle) has alignment through the width of the sample (shorter direction), and this alignment is denoted as alignment in the z-direction. However, in the bi-directional sample (square), there are two directions of filler alignment, which are  $90^\circ$  from one another, effectively creating a mesh pattern. Alignments are in the x and z-direction. The bi-directional samples were fabricated in layers. An initial layer was fabricated within the mold with fillers aligned in one direction. The electrodes were then moved to create alignment perpendicular to that of the first layer. Another layer of resin-filler solution was added, and fillers aligned. Figure 13 shows images of the individual layers of a prepared sample as well as an overlapping view of the layers which shows alignment in both directions, taken by a digital microscope. Filler loadings for the sample shown are high enough to show alignment, but are too low to create continuous chains across the entire part.



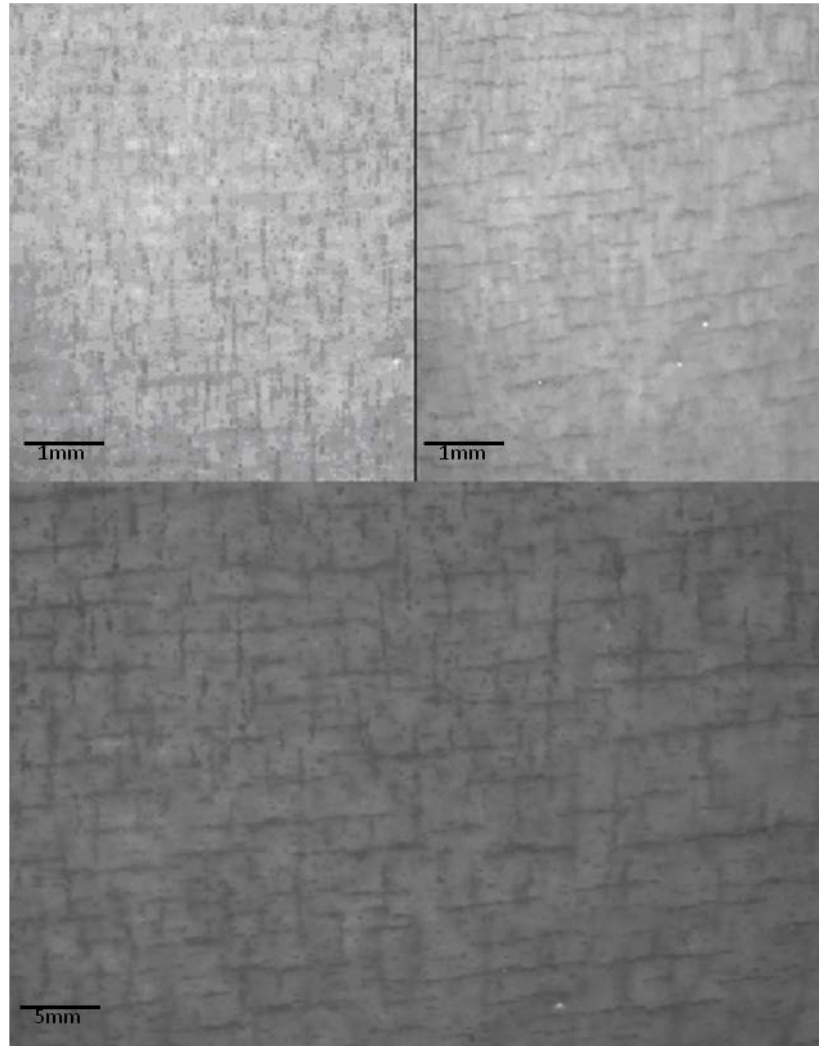


Figure 13. Images of a bi-directional sample taken by a digital microscope, (c.w. from top left):  $0^\circ$  orientation,  $90^\circ$  orientation, bi-directional alignment overlapping view

This creates samples that represent traditional fiber reinforced polymer composites on a microscopic scale. Just like in traditional fiber composites with non-woven, bi-directional orientations, one layer is applied with the fillers aligned in one orientation, which could be described as alignment in the  $0^\circ$  (or origin) direction. The next layer is then applied with the fillers aligned in the perpendicular or  $90^\circ$  direction.

---

### 3. Results and Conclusions

---

The experimental FALCom process has shown the capability to fabricate multi-layered particulate reinforced polymer composites with controlled filler orientation like that of figure 14. It has been shown that the selected fillers can be aligned in order to create pseudo-fiber support structures. In future experimentation, these structures may be used for structural, electrical or thermal manipulation of a polymer composite.

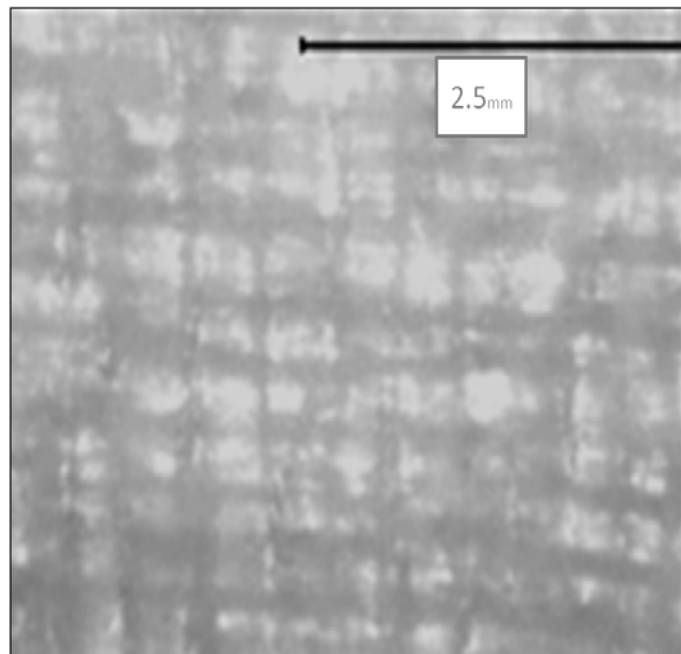


Figure 14. Laminar micro-composite; aluminum micro-particles aligned in a  $0^\circ$ ,  $90^\circ$  orientation in an acrylic matrix.

This study was conducted to facilitate a proof of concept for the FALCom technology, and therefore a limited number of specimens were fabricated for each sample set. In the future, an in-depth study will be conducted into the mechanical properties of FALCom fabricated composite structures. Preliminary results from mechanical characterization of the composite samples with the bi-directional alignments have shown to increase the flexural modulus by up to 24% over those with randomly oriented fillers. Photoelastic response of FALCom specimens will also be evaluated in the future. A preliminary example of that evaluation can be seen in figure 15.



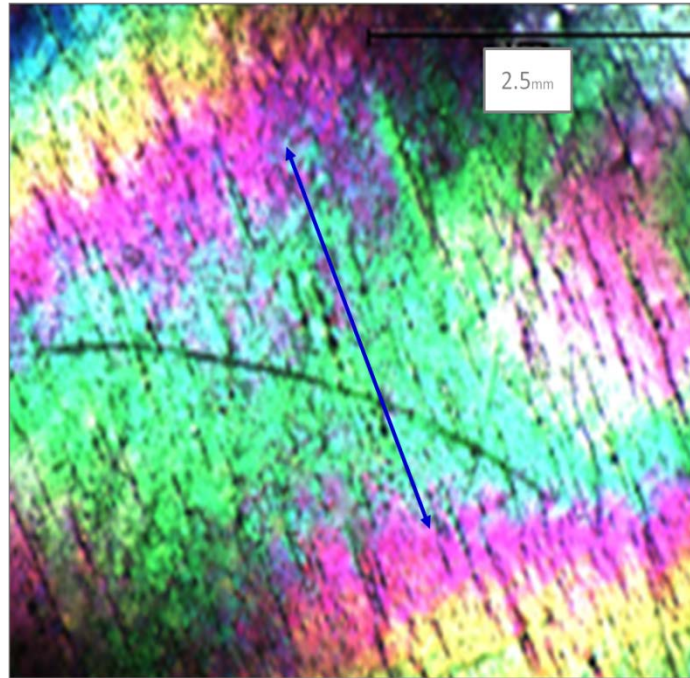


Figure 15. Example of photoelastic response of a unidirectional micro-composite with carbon particulate chains in an acrylic matrix. An arrow denotes direction of alignment.

The FALCom processing technology, a process for creating multi-directional nano- and micro-composites, has been realized. This study was conducted with a bench top version of the FALCom processing technology with a fabrication envelope of approximately one cubic inch. A large-scale FALCom machine is being constructed currently that will have a working volume of approximately one cubic foot. This machine will be used to determine if the technology is applicable for the fabrication of three-dimensionally reinforced rapid prototype composites, and will continue to support research and analysis of micro-composites.

---

## 4. References

---

1. Holmes, L. R. Jr. Multi-Directional Field Aided Manipulation of Fillers in Polymer Composites, Master of Science Thesis, University of Wisconsin-Madison, 2008.
2. Maxwell, J. C. *A Treatise on Electricity and Magnetism* Vol. 1. Clarendon Press: Oxford, 1880.
3. Pohl, H. A. The Motion and Precipitation of Suspensoids in Divergent Electric Fields. *Journal of Applied Physics* **1951**, 22 (7), 869–871.
4. Pohl, H. A. *Dielectrophoresis the Behavior of Neutral Matter in Nonuniform Electric Fields*. Cambridge University Press Cambridge, 1978.
5. Happel, J.; Brenner, H. *Low Reynolds Number Hydrodynamics (with special applications to particle media)*. Prentice-Hall: New Jersey, 1965.
6. Happel, J.; Brenner, H. *Low Reynolds Number Hydrodynamics*. Martinus Nijhoff Publishers: Dordrecht, The Netherlands, 1983.
7. Tierney, M. J.; Martin, C. R. Electoreleasing Composite Membranes for Delivery of Insulin and Other Biomacromolecules. *J. Electrochem. Soc.* **1990**, 137, 2005–06.
8. Norman, D. A.; Robertson, R. E. Rigid-Particle Toughening of Glassy Polymers. *Polymer* **2003**, 44, 2351–2362.
9. Bowen, C. P.; Newnhan, R. E.; Randall, C. A. Dielectric Properties of Dielectrophoretically Assembled Particulate-Polymer Composites. *J. Mater. Res* **1998**, 13 (1), 205–210.
10. Bowen, C. P.; Newnhan, R. E. et al. A Study of the Frequency Dependence of the Dielectrophoretic Effect in Thermoset Polymers. *J. Mat. Res.* **1997**, 12 (9), 2345–2356.
11. Kim, G. H.; Shkel, Y. M.; Rowlands, R. E. Field-Aided Micro-Tailoring of Polymeric Nanocomposites. *In Proceedings of SPIE*, 2003.
12. Shkel, Y. M.; Kim, G. H.; Rowlands, R. E. Analysis of Functionally Graded Composites Fabricated by Field Aided Micro-Tailoring Techniques, *In Proceedings of the International Symposium on Experimental Mechanics*, Taipei, Taiwan, 2002.
13. Kim, G. H.; Moeller, D. K., Shkel, Y. M. Functionally Graded Polymeric Composites With Field-Aided Micro-Tailored Structure. *In ASME International Engineering Congress and R&D Expo (IMECE)*, Washington, DC, 2003.
14. Rud, J. A. *Manufacturing and Characterization of Micro-Tailored Composites*, M.S. Thesis, University of Wisconsin-Madison, 2006.

15. Landau, L. D.; Lifshitz, E. M. *Electrodynamics of Continuous Media*; Pergamon Press: Oxford, pp. 368–376, 1960.
16. Pohl, H. A. Some Effects of Nonuniform Fields on Dielectrics. *Journal of Applied Physics* **1958**, 29 (8) 1182–1188.
17. Kim, G. H., Moeller, D. K., Shkel, Y. M. Orthotropic Polymer Composites with Microstructure Tailored by Electric Field. *Journal of Composite Materials* **2004**, 38 (21) 1895–1909.
18. Kim, G. H. *Field Aided Technology for Local Micro-Tailoring of Polymeric Composites with Multi-Functional Response*, PhD. Thesis, University of Wisconsin-Madison, 2003.
19. Kim, G. H.; Shkel, Y. M. Polymeric Composites Tailored by Electric Field. *Journal of Material Research* **2004**, 19 (4) 1164–1174.

NO. OF  
COPIES ORGANIZATION

1 DEFENSE TECHNICAL  
(PDF INFORMATION CTR  
only) DTIC OCA  
8725 JOHN J KINGMAN RD  
STE 0944  
FORT BELVOIR VA 22060-6218

1 DIRECTOR  
US ARMY RESEARCH LAB  
IMNE ALC HRR  
2800 POWDER MILL RD  
ADELPHI MD 20783-1197

1 DIRECTOR  
US ARMY RESEARCH LAB  
RDRL CIO LL  
2800 POWDER MILL RD  
ADELPHI MD 20783-1197

NO. OF  
COPIES ORGANIZATION

ABERDEEN PROVING GROUND

5 HC DIR USARL  
RDRL WMM A  
J M GARDNER  
L R HOLMES, JR.  
Z J LARIMORE  
J P WOLBERT

INTENTIONALLY LEFT BLANK.